

Chapter 2

Types of Wind Turbines

Ich halte dafür, daß das einzige Ziel der Wissenschaft darin besteht, die Mühseligkeit der menschlichen Existenz zu erleichtern (Presumably for the principle that science's sole aim must be to lighten the burden of human existence, B. Brecht) [1].

Equation (1.5) from Chap. 1 may also be used to define an efficiency or *power coefficient* $0 \leq c_P \leq 1$:

$$c_P = \frac{P}{\frac{\rho}{2} A_r \cdot v^3}. \quad (2.1)$$

Wind turbine aerodynamic analysis frequently involves the derivation of useful equations and numbers for this quantity. Most (in fact, almost all) wind turbines use *rotors* which produce *torque or* moment of force

$$M = P/\omega. \quad (2.2)$$

with $\omega = \text{RPM} \cdot \pi/30$ the angular velocity. Comparing tip speed $v_{\text{Tip}} = \omega \cdot R_{\text{Tip}}$ and wind speed, we have

$$\lambda = v_{\text{Tip}}/v_{\text{wind}} = \frac{\omega \cdot R_{\text{Tip}}}{v_{\text{wind}}}. \quad (2.3)$$

the tip speed ratio (TSR). Figure 2.1, sometimes called the *map of wind turbines*, gives an overview of efficiencies as a function of non-dimensional RPM. The numbers are estimated efficiencies only. A few remarks are germane to the discussion. From theory (Betz, Glauert), there are clear efficiency limits, but no theoretical maximum TSR. In contrast, the semiempirical curves for each type of wind turbine have a clearly defined maximum efficiency value.

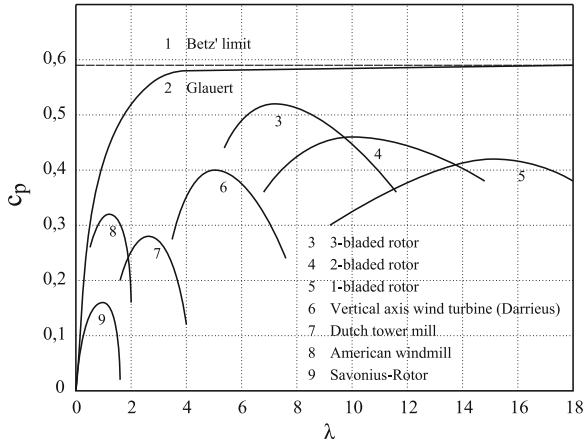


Fig. 2.1 Map of wind turbines

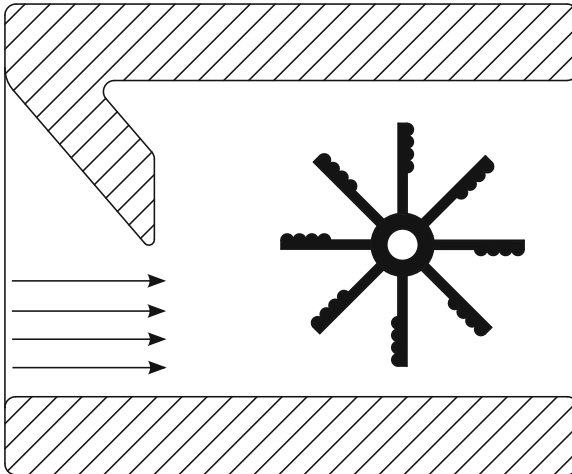


Fig. 2.2 Persian windmill

2.1 Historical and State-of-the-Art Horizontal Axis Wind Turbines

The wind energy community is very proud of its long history. Some aspects of this history are presented in [2, 3]. Apparently, the oldest one [3] is the so-called *Persian* windmill (Fig. 2.2). It was first described around 900 AD and is viewed from our system of classification (see Sect. 2.6) as a drag-driven windmill with a vertical axis of rotation.

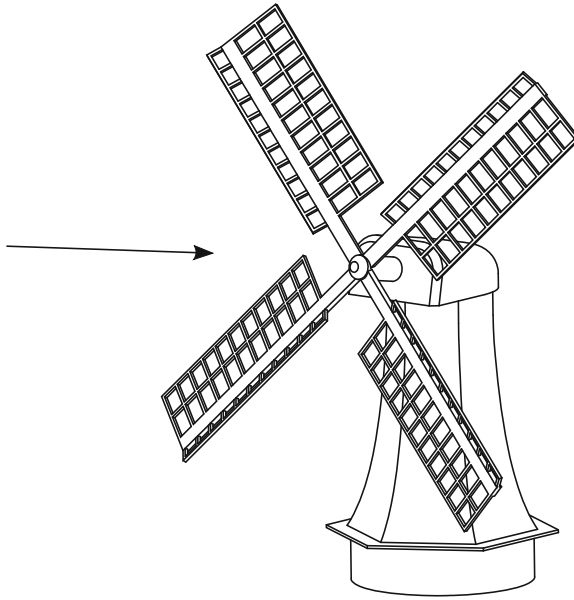


Fig. 2.3 Dutch windmill

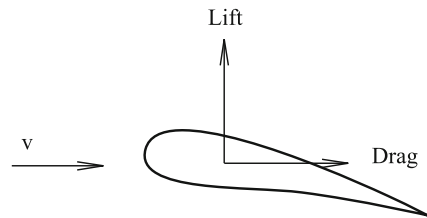
Somewhat later, the *Dutch* windmill appeared as the famous *Windmill Psalter* of 1279 [3], see Fig. 2.3. This represented a milestone in technological development: The axis of rotation changed from vertical to horizontal. But also from the point of view of aerodynamics, the Dutch concept began the slow movement toward another technological development: lift replacing drag. These two types of forces simply refer to forces perpendicular and in-line with the direction of flow. The reason this is not trivial stems from *D'Alembert's Paradox*:

Theorem 2.1 *There are no forces on a solid body in an ideal flow regime.*

We will continue this discussion further in Chap. 3. These very early concepts survived for quite a few centuries. Only with the emergence of electrical generators and airplanes were these new technologies adapted, in the course of a few decades, to what is now called the standard horizontal axis wind turbine:

- horizontal axis of rotation
- three bladed
- driving forces mainly from lift
- upwind arrangement of rotor; tower downwind
- variable speed/constant TSR operation
- pitch control after rated power is reached.

Fig. 2.4 Lift and drag forces on an aerodynamic section



2.2 Non-Standard HAWTs

With this glimpse of what a *standard* wind turbine should be, everything else is *non-standard*:

- **no** horizontal axis of rotation
- number of blades other than three (one, two, or more than three)
- drag forces play important role
- downwind arrangement of rotor; tower upwind
- constant speed operation
- so-called **stall** control after rated power is reached.

From these characteristics, we may derive a large number of different designs. Only a few of them became popular enough to acquire their own names (Fig. 2.4):

The *American* or *Western-type* turbine [3]. Chapter 1 uses a very high (10–50) number of blades which in most cases are flat plates with a small angle between plane of rotation and chord. These turbines were used mainly in the second half of the nineteenth century, see Fig. 2.5.

The *Danish Way* of extracting wind energy [4] used most of the now classical properties with a fixed-pitch blade arrangement and a constant RPM operation mode. The development of this design philosophy started in the 1940s and died off slowly in the 1990s.

2.3 Small Wind Turbines

Small wind turbines are defined by IEC [5] as a wind turbine with a rotor swept area no greater than 200 m². Therefore, the diameter is limited to 16 m. However, most of them have much smaller diameters starting at about 1 m. More can be found in [6]. Figure 2.6 gives an account of scaling. The main problem with safety approval of [5] is that it offers two very different methods:

- the usual aero elastic simulation modeling,
- a simplified load model.

The first one implies the same amount of work as for a state-of-the-art turbine and is not economical in most cases. The second procedure is much easier (see [6]) but at the

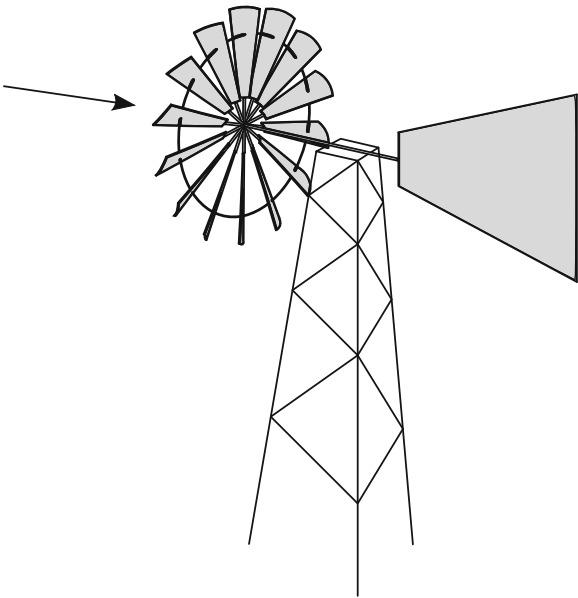


Fig. 2.5 American or western windmill

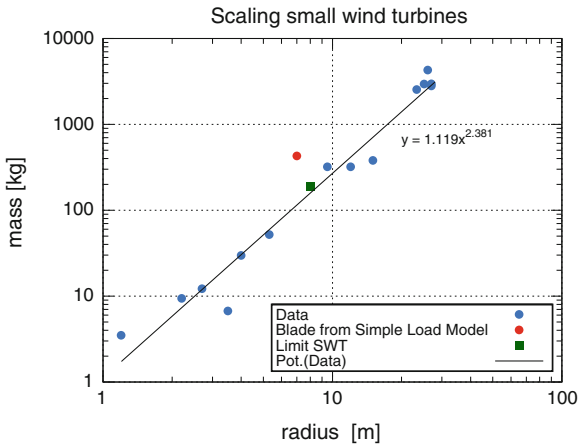


Fig. 2.6 Scaling of blade masses of smaller wind turbines

expense of exceedingly high safety factors. As an example, the required blade-mass for the simple load model is shown in Fig. 2.6. The mass required by the simple load model has to be more than 300 kg, compared to only 120 kg for a blade designed without these high safety factors.

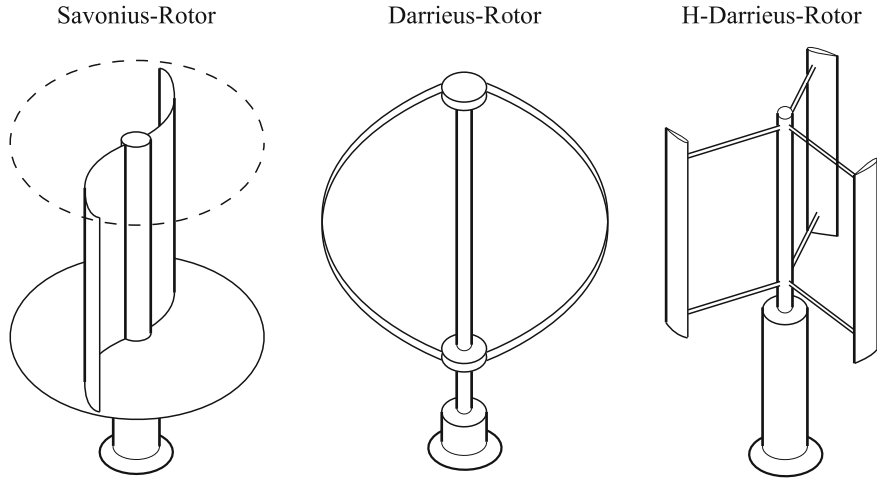


Fig. 2.7 Types of vertical axis wind turbines

2.4 Vertical Axis Wind Turbines

As was explained earlier, vertical axis windmills and the subsequent vertical axis wind turbines seem to be older than those with an horizontal axis of rotation. Mainly due to the inventions of Darrieus [7] and Savonius [8]¹ interest in these vertical turbines was renewed in the early twentieth century. Then, after the first so-called oil crisis in the beginning of the 1970s, many US [9–12] and German [13–19] vertical turbine development efforts were undertaken which lasted until the 1990s, while HAWTs also progressed. A summary may be found in [20]. Now, after some 20 years of dormancy, interest in VAWTs seems to be returning slowly, see for example [21] (Fig. 2.7).

One of the big advantages is the independence of directional change in wind. See Fig. 2.8 for a typical distribution of wind direction at a typical site. Also, heavy components may be installed close to the ground, as illustrated in Fig. 2.9. The largest VAWT manufactured so far was the so-called Éole-C made in Canada. Its height was about 100 m, the rotating mass was 880 metric tons, and the rated power was supposed to be 4 MW. Unfortunately, due to severe vibration problems, the rotational speed was limited to such low values that only 2 MW was reached [20].

It has to be noted that the flow mechanics behind these designs (see Problems 6.1 and 6.2 in Chap. 6) is much more interesting—but also more complicated—due to fact that the sphere of the influence of the rotor is modeled as a real volume and not a 2D disk as is assumed for the HAWT actuator disk model. Therefore, at least for each half revolution, the blades are operating in a wake, meaning that load fluctuations have a much greater influence on the blades. The resulting so-called aerodynamic

¹ A more detailed discussion can be found in Sect. 2.6.

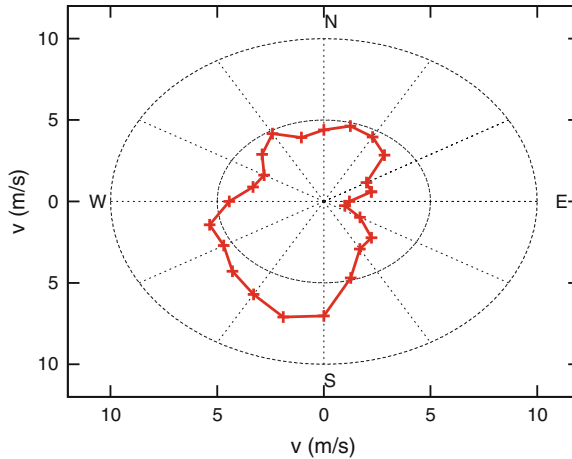


Fig. 2.8 Typical wind direction distribution near Hamburg at 10 m height

fatigue loads for a VAWT rotor blade are much higher and are one of the reasons that VAWTs are much more prone to earlier failure of components—mostly at joints—than are HAWTs.

One way out of this difficulty is the so-called *Gyro-Mill* or articulated VAWT [22], where the pitch angle (the angle of the chord line in relation to the circumference) is changed periodically so that—in an ideal case—the driving force remains almost constant (Fig. 2.10).

2.5 Diffuser Augmented Wind Turbines

As we have seen, the power contained in the wind is proportional to the swept area. An obvious extension of this concept is to look for *wind-concentrating* devices resembling a cone or funnel, see Fig. 2.11. Such devices are very common in wind turbines and are called draft tubes or suction tubes. From first principles of fluid mechanics, the **exit** area of such a device has to be larger than the inflow area. At a glance, this is clearly counterintuitive. Then, by closer inspection of the basic laws of conservation of mass and energy—called *Bernoulli's law*—it follows that an increase in mass flow proportional to the area ratio $A_{\text{exit}}/A_{\text{inflow}}$ is possible if the flow follows the contour of the cone.

Unfortunately, nature is not that generous. The increase in diameter has to be very moderate. To be more precise, opening angles less than 10° have to be used to avoid what is called flow separation. It immediately follows that, to have reasonable area ratios, we have to use very long diffusers with very large weights. The engineering task then is to find a reasonable compromise—if possible at all. Serious work started in 1956 by Liley and Rainbird [23] and efforts up to 2007 are summarized by van Bussel [24]. Some applications to small wind turbines may be found at [25].



Fig. 2.9 Dornier's Eole-D, height = 20 m, $P_{\text{rated}} = 50$ kW. Reproduced by permission of EnBW Windkraftprojekte GmbH, Stuttgart, Germany

2.6 Drag-Driven Turbines

Drag was defined earlier as a force on a structure subjected to a stream of air **in line** with the flow, see Fig. 2.4. We therefore define a simple number, the *drag coefficient* (Fig. 2.12):

$$c_D := \frac{D}{\frac{\rho}{2} \cdot A_r \cdot v^2}. \quad (2.4)$$

Fig. 2.10 Example of a DAWT, wind from *right*

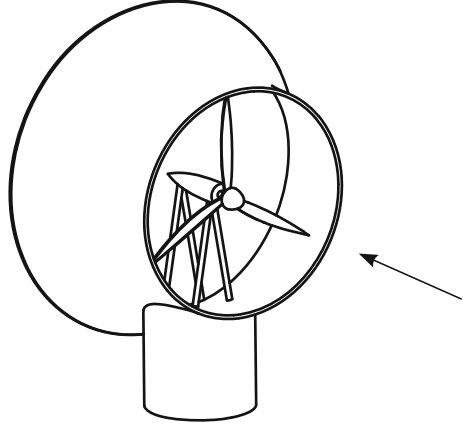
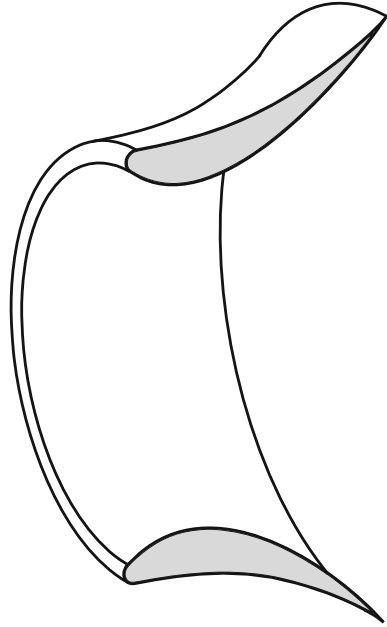


Fig. 2.11 Cross section of a diffuser or ring-wing



To imagine this, we consider at first a simply translating sail of velocity u and Area $A = c \cdot \ell$ and v the wind velocity as usual. The power $P = D \cdot u$, is using Eq. (2.4):

$$P = \frac{\rho}{2}(v - u)^2 \cdot c_D \cdot c \cdot \ell \cdot u. \quad (2.5)$$

Now using $P_{\text{wind}} = \frac{\rho}{2}v^3$, we have:

$$c_P = c_D (1 - u/v)^2 (u/v). \quad (2.6)$$

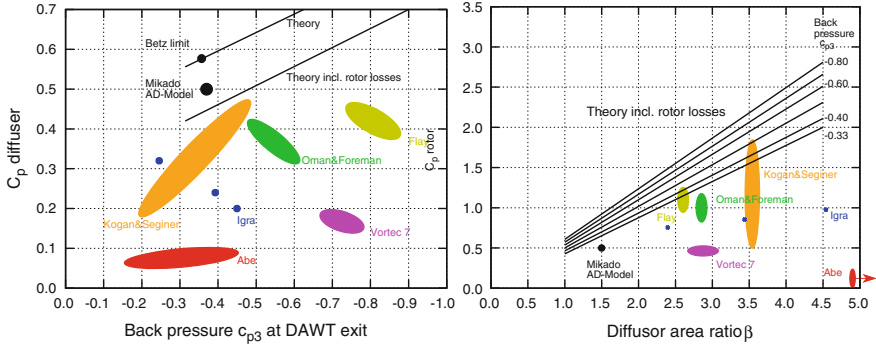


Fig. 2.12 Collected performance data for diffusers, from van Bussel (2007)

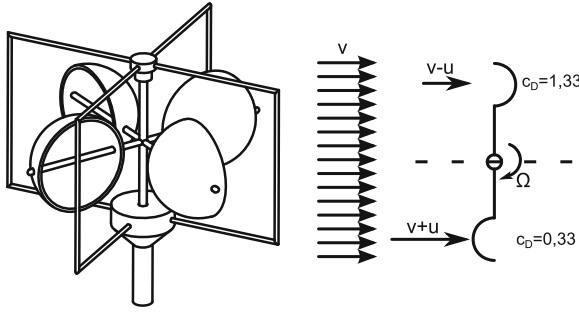


Fig. 2.13 Drag-driven turbines

Setting $a := u/v$ and solving for a by making $\frac{dc_P}{da} = 0$, we see that the maximum power of such a *drag-driven vehicle* may not exceed

$$c_P^{\max, D} = \frac{4}{27} \cdot c_D \text{ at } a = \frac{1}{3} \quad (2.7)$$

$c_P^{\max, D} \approx 0.3$ if $\mathbf{u} = \mathbf{1/3} \mathbf{v}$. For example, a sailing boat at wind force 7 (Beaufort ≈ 30 knots ≈ 16.2 m/s) may not travel faster than 10 Knots. If it has 30-m^2 sail area, the maximum power will be $P = 24$ kW.

The next step is to discuss the *Persian wind mill* or the closely related anemometer, see Fig. 2.13. The idea is to use a specially shaped body (semi-sphere) which has different c_D when blown from one side or the other. A common pair of values for c_D is $c_{D+} = 1.33$ and $c_{D-} = 0.33$. We then arrive at:

$$F_+ = c_{D+} \cdot \frac{\rho}{2} A_r (u - \Omega r) \quad (2.8)$$

$$F_- = c_{D-} \cdot \frac{\rho}{2} A_r (u + \Omega r) \text{ and finally} \quad (2.9)$$

$$c_P = (F_+ - F_-) \cdot v / A_r = \lambda \left(c_1 - c_2 \cdot \lambda + c_1 \cdot \lambda^2 \right) \quad (2.10)$$

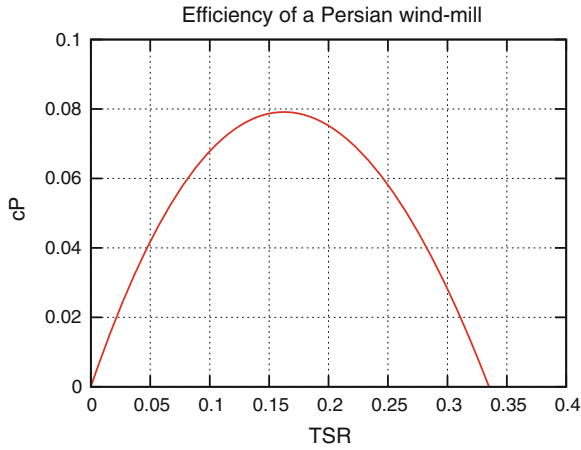


Fig. 2.14 Performance curve of an anemometer

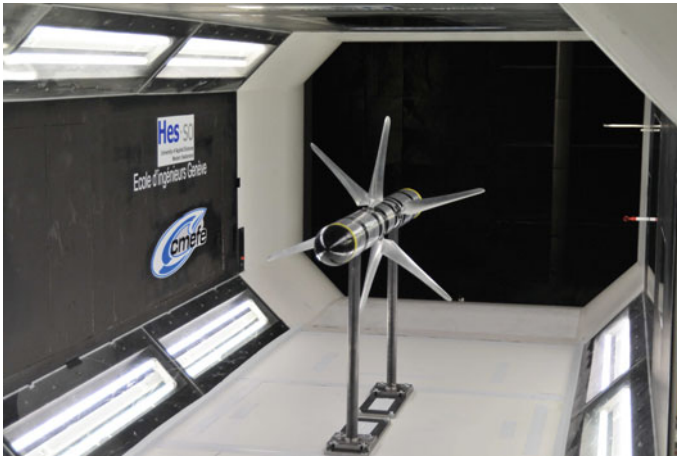


Fig. 2.15 Model of a counter-rotating wind turbine in a wind tunnel, diameter = 800 mm. Reproduced with permission of HEIG-VD, Iverdon-les-Bains, Switzerland

with $c_1 = c_{D+} - c_{D-}$ and $c_2 = 2 \cdot (c_{D+} + c_{D-})$. Figure 2.14 shows that a very small efficiency at very low TSR ($c_{D+} = 1.33$ and $c_{D-} = 0.33$).

2.7 Counter-Rotating Wind Turbines

For some ship propellers and helicopters, there have been efforts to use to rotors rotating in opposite direction to improve the efficiency of the whole system. Unlike propellers and helicopters, swirl losses (see Sect. 5.2) appear to be small in wind

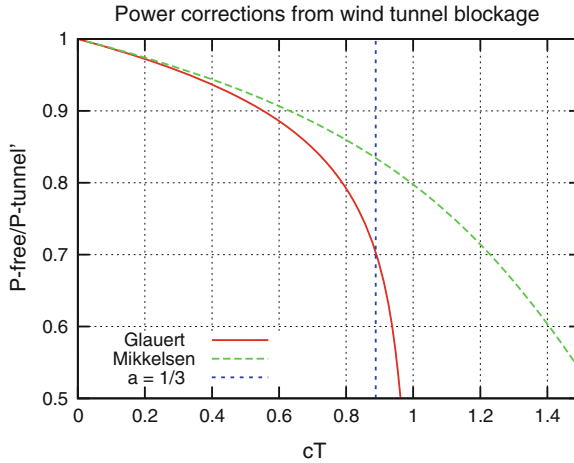


Fig. 2.16 Blockage corrections from Glauert [28] and Mikkelsen [29]

turbines. Nevertheless, many investigations of swirl losses [26, 27] have been undertaken. Figure 2.15 shows a model wind turbine which was evaluated during a wind tunnel experiment in 2009 in Geneva. Clearly, an improvement of about 10 % was seen in performance but somewhat obscured by a rather large and uncertain blockage correction, which is of utmost importance to consider when comparing wind tunnel experiments with a freely expanding wake. From a theoretical point of view, this type of turbine is very interesting, because a swirl component does not have to be included. We will come back to this point in Chap. 6 (Fig. 2.16).

2.8 Concluding Remarks

We finish this chapter by noting that a myriad of other turbine types exist, some of which are based on very specific fluid mechanics principles or ideas. Even a pinwheel (toy) turbine was investigated experimentally [30]. The reader may consult the older literature [31, 32] for many highly entertaining examples.

2.9 Problems

Problem 2.1 Derive Eq. 2.10 and find an expression for c as a function of c_{D+} and c_{D-} .

Problem 2.2 Estimate the increase of power for a DAWT with the following properties: $D_{\text{Rotor}} = 1\text{ m}$, $D_{\text{exit}} = 1.17\text{ m}$ and efficiency of diffuser $\eta_{\text{diff}} = 0.85$.

Problem 2.3 Determine if a counter-rotating turbine consists of one turbine or two and give your reasons.

References

1. Brecht B (2008) *Life of Galileo*. Penguin Classics, London, UK, Reprint
2. Beurskens J (2014) History of wind energy, chapter 1 of: understanding wind power technology. In: Schaffarczyk AP (ed), Wiley, Chichester
3. Spera D (ed) (2009) *Wind turbine technology*, 2nd edn. ASME Press, New York
4. Nossen P-O et al (2009) *Wind power—the Danish way*. The Poul la Cour Foundation, Askov
5. International Electro-technical Commission (2011) IEC 61400–2 Ed. 3, Small wind turbines, Geneva (draft)
6. Wood D (2011) *Small wind turbines*. Springer, London
7. Darrieus GJM (1931) Turbine having its rotating shaft transverse to the flow field of the current, US Patent 1 835 018
8. Savonius SJ (1930) Windrad mit zwei Hohlflügeln, deren Innenkanten einen zentralen Wind-durchlaßspalt freigeben und sich übergreifen. Patentschrift Nr 495:518
9. Ashwill TD (1992) Measured data for the Sandia 34 m vertical axis wind turbine, SAND91-228, Albuquerque, New Mexico
10. Carne TG et al (1982) Finite element analysis and modal testing of a rotating wind turbine, SAND82-0345. Albuquerque, New Mexico
11. Homicz GF (1991) Numerical simulation of VAWT stochastic aerodynamic loads produced by atmospheric turbulence: VAWT-SAL code, SAND91-1124. Albuquerque, New Mexico
12. Oler JW et al (1983) Dynamic stall regulation of the darrieus turbine, SAND82-7029. Albuquerque, New Mexico
13. Bankwitz H et al (1975) Entwicklung einer Windkraftanlage mit vertikaler Achse (Phase I), Abschlußbericht zum Forschungsvorhaben ET-4135 A. Dornier System GmbH, Friedrichshafen
14. Binder G et al (1978) Entwicklung eines 5,5 m Ø-Windenenergiekonverters mit vertikaler Drehachse (Phase II), Abschlußbericht zum Forschungsvorhaben T-79-04. Dornier System GmbH, Friedrichshafen
15. Dekithsch A et al (1982) Entwicklung eines 5,5 m Durchmesser-Windenenergiekonverters mit vertikaler Drehachse (Phase III), Abschlußbericht zum Forschungsvorhaben T-82-086. Dornier System GmbH, Friedrichshafen
16. Eckert L, Seeßelberg C (1990) Analyse und Nachweis der 50 kW—Windnergieanlage (Typ Darrieus), MEB 55/90, internal report. Dornier GmbH, Immenstaad, Germany
17. Henseler H, Eole-D MW (1990) Technologieprgramme Darrieus Windenergieanlagen Anpaßentwicklung, 2. Abschlußbericht zum Forschungsvorhaben 0328933 P, Dornier GmbH, Immenstaad, Germany
18. Meier H, Richter B (1988) Messungen an der Windkraftanlage DAWI 10 und Vergleich mit theoretischen Untersuchungen, Abschlußbericht WE-4/88 zum Forschungsvorhaben 03E–8384-A. Germanischer Lloyd, Hamburg
19. NN (1990) Technische Anlage zum Angebot Nr. 3026-0-90, Lieferung und Montage einer 2,25 MW Darrieus-Windenenergieanlage EOLE-D, Dornier GmbH, Friedrichshafen
20. Paraschivoiu I (2002) *Wind turbine design, with emphasis on Darrieus concept*. Polytechnic International Press, Montreal, Canada
21. Ferreira CS (2009) The near wake of the VAWT, PhD. thesis, TU Delft, The Netherlands
22. Clausen RS, Søndersby IB, Andkjær JA (2006) Eksperimentel og Numerisk Undersøgelse af en Gyro Turbine, Plyteknisk Midtvejsprojekt, Institut for Mekanik, Energi og Konstruktion, The Danish Technical University, Lyngby

23. Lilley GM, Rainbird WJ (1956) A preliminary report on the design and performance of ducted windmills, report no. 102, Cranfield, College of Aeronautics, UK
24. van Bussel GJW (2007) The science of making more torque from wind: Diffuser experiments and theory revisited. *J Phys Conf Ser* 75:012010
25. Schaffarczyk AP (2007) Auslegung einer Kleinwindanlage mit Mantel, aerodynamischen Leistungsdaten, Optimierung des Diffusers, unveröffentlichte und vertrauliche Berichte Nr bf 49, 50 und 51
26. Herzog R, Schaffarczyk AP, Wacinski A, Zürchner O (2010) Performance and stability of a counter-rotating windmill using a planetary gearing: measurements and simulation, In: *Proceedings of EWEC 2010*, Warsaw, Poland
27. Shen WZ, Zakkam VAK, Sørensen JN, Appa K (2007) Analysis of counter-rotation wind turbines, *J Phys Conf Ser* 75:012003
28. Glauert H (1926) *The elements of aerofoil and airscrew theory*, Repr, 2nd edn. Cambridge University Press, Cambridge
29. Mikkelsen R (2003) *Actuator disk methods applied to wind turbines*, PhD thesis, The Technical University of Denmark, Lyngby
30. Nemoto Y, Ushiyama I (2003) Wind engineering. *Exp Study Pinwheel-Type Wind Turbine* 27(2):227–235
31. Molly J-P (1990) *Windenergie—theorie, anwendung, messung*, 2nd edn. Verlag C.F. Müller Karlsruhe, Germany
32. de Vries O (1979) *Fluid dynamic aspects of wind energy conversion*, AGARDograph, No. 243, Neuilly sur Seine, France

Introduction to Wind Turbine Aerodynamics

Schaffarczyk, A.P.

2014, XXII, 265 p. 233 illus., 136 illus. in color.,

Hardcover

ISBN: 978-3-642-36408-2